Arteriosclerosis, Thrombosis, and Vascular Biology

BASIC SCIENCES

Novel *Myh11* Dual Reporter Mouse Model Provides Definitive Labeling and Identification of Smooth Muscle Cells—Brief Report

Jian Ruan,* Lu Zhang,* Donghua Hu,* Xianghu Qu, Fan Yang, Fuxue Chen, Xiangqin He, Jian Shen, Kunzhe Dong, Megan Sweet, Christina Sanchez, Deqiang Li, Weinian Shou, Jiliang Zhou, Chen-Leng Cai

OBJECTIVE: *Myh11* encodes a myosin heavy chain protein that is specifically expressed in smooth muscle cells (SMCs) and is important for maintaining vascular wall stability. The goal of this study is to generate a *Myh11* dual reporter mouse line for definitive visualization of MYH11$^+$ SMCs in vivo.

APPROACH AND RESULTS: We generated a *Myh11* knock-in mouse model by inserting *LoxP-nlacZ-4XpolyA-LoxP-H2B-GFP-polyA-FRT-Neo-FRT* reporter cassette into the *Myh11* gene locus. The nuclear (n) *lacZ-4XpolyA* cassette is flanked by 2 *LoxP* sites followed by H2B-GFP (histone 2B fused green fluorescent protein). Upon Cre-mediated recombination, *nlacZ-stop* cassette is removed thereby permitting nucleus localized H2B-GFP expression. Expression of the nuclear localized lacZ or H2B-GFP is under control of the endogenous *Myh11* promoter. Nuclear lacZ was expressed specifically in SMCs at embryonic and adult stages. Following germline Cre-mediated deletion of nuclear lacZ, H2B-GFP was specifically expressed in the nuclei of SMCs. Comparison of nuclear lacZ expression with *Wnt1^{Cre}* and *Mef2c^{Cre}* mediated-H2B-GFP expression revealed heterogenous origins of SMCs from neural crest and second heart field in the great arteries and coronary vessels adjacent to aortic root.

CONCLUSIONS: The *Myh11* knock-in dual reporter mouse model offers an exceptional genetic tool to visualize and trace the origins of SMCs in mice.

GRAPHIC ABSTRACT: A graphic abstract is available for this article.

Key Words: knock-in ■ Myh11 ■ reporter mouse ■ smooth muscle cells

Blood vessels are a highly organized tissue composed of smooth muscle cells (SMCs), endothelial cells, fibroblasts, resident immune cells, and extracellular matrix.[1] The vascular SMCs contribute to most of the arterial wall. As an essential component, vascular SMCs play a vital role in vessel contraction, blood pressure regulation, and blood flow distribution.[2] In response to vascular injuries, vascular SMCs can switch from a contractile phenotype to a proliferative phenotype, thereby participating the repairing process to maintain proper structure and function of the arteries.[3,4]

Understanding how SMCs develop from the progenitor cells and how they regenerate upon injury are fundamental questions in vascular biology. The *Myh11* gene, encoding MYH11 (myosin heavy chain 11; also known as SM-MHC [smooth muscle myosin heavy chain]), a major component of the contractile apparatus, is a specific marker of mature SMCs.[5] MYH11 has been widely used as a definitive marker for SMCs during embryonic

Correspondence to: Chen-Leng Cai, PhD, Department of Pediatrics, Indiana University School of Medicine, 1044 W. Walnut St, R4-372, Indianapolis 46202, Indiana, Email chenleng@iu.edu; or Jiliang Zhou, MD, PhD, Department of Pharmacology & Toxicology, Medical College of Georgia, Augusta University, 1459 Laney Walker Blvd, Augusta 30912, Georgia, Email jizhou@augusta.edu

*These authors contributed equally to this article.

The Data Supplement is available with this article at https://www.ahajournals.org/doi/suppl/10.1161/ATVBAHA.120.315107.

For Sources of Funding and Disclosures, see page 821.

Arterioscler Thromb Vasc Biol is available at www.ahajournals.org/journal/atvb

Nonstandard Abbreviations and Acronyms

GFP	green fluorescent protein
H2B-GFP	histone 2B fused green fluorescent protein
MYH11	myosin heavy chain 11
nlacZ	nuclear lacZ
SMC	smooth muscle cell
SM-MHC	smooth muscle myosin heavy chain

and postnatal development.[4,6] Mutations in *MYH11* gene can disrupt SMC contractile function and lead to thoracic aortic aneurysms and aortic dissections,[7,8] a major cause of morbidity and mortality in humans. Moreover, patients with intestinal neoplasia also show *MYH11* frameshift or point mutations which impact the balance of cellular energy and kinetics of motor function.[9] Despite these extensive functional studies of MYH11, detecting endogenous *Myh11* expression has largely relied on immunostaining with MYH11 antibody or in situ hybridization to detect *Myh11* mRNA. RNA in situ hybridization is cumbersome and relatively insensitive and immunologic staining largely relies on the specificity and efficacy of antibodies which are often not well characterized. These methods can sometimes become difficult when SMCs are phenotypically changed in pathological conditions. Therefore, there is an urgent need to generate a genetic tool that faithfully mimics *Myh11* gene expression and allows a better visualization of SMCs during development and disease.

Here we created a novel *Myh11* dual reporter mouse model by knocking-in a *nlacZ/H2B-GFP* expression cassette into the *Myh11* locus. We verified that the reporter genes in *Myh11*$^{nlacZ\text{-}H2B\text{-}GFP/+}$ animal mark SMCs from embryonic stage to adulthood. This mouse line offers a robust genetic tool not only to monitor *Myh11* expression, but also to trace SMC origins in the physiological and pathological conditions.

MATERIALS AND METHODS

The data that support the findings of this study are available from the corresponding authors upon reasonable request.

The *Myh11*$^{nlacZ\text{-}H2B\text{-}GFP/+}$ knock-in mouse model was generated by targeting *LoxP-nlacZ-4XpolyA-LoxP-H2B-GFP-polyA-FRT-Neo-FRT* cassette into *Myh11* genomic locus (6-bp upstream of the ATG; Figure IA in the Data Supplement). X-gal staining and immunostaining of mouse tissues were performed as previously described.[10,11] Use of the experimental animals is approved by the Institutional Animal Care and Use Committee and Biosafety committee at Indiana University and Augusta University in accordance with the National Institutes of Health guidelines. Both male and female mice were used in this study. A detailed, expanded method section is included in the Data Supplement.

Highlights

- To better visualize *Myh11* expression in smooth muscle cells (SMCs), we generated a dual reporter mouse line by inserting *LoxP-nlacZ-stop-LoxP-H2B-GFP* cassette into the *Myh11* locus.
- The lacZ and GFP (green fluorescent protein) expression is restricted in the SMC nuclei and faithfully labels SMCs from embryonic stage to adulthood in the reporter mice.
- *Wnt1*^{Cre} and *Mef2c*^{Cre} mediated GFP expression in the dual reporter mice revealed heterogenous origins of SMCs in the great arteries and the coronary vessels adjacent to aortic root.
- The *Myh11* dual reporter mouse model offers an exceptional genetic tool to detect SMCs and trace their developmental origins.

RESULTS

Generation of *Myh11*$^{nlacZ\text{-}H2B\text{-}GFP/+}$ Knock-In Mouse and Characterization of nlacZ Expression in the Reporter Line

We generated *Myh11*$^{nlacZ\text{-}H2B\text{-}GFP/+}$ mouse model by inserting *LoxP-nlacZ-4XpolyA-LoxP-H2B-GFP-polyA-FRT-Neo-FRT* cassette into the start codon region of *Myh11* through homologous recombination (Figure 1A and Figure IA in the Data Supplement). The nuclear *lacZ (nlacZ)-4XpolyA* stop cassette (*nlacZ-4XpolyA*) is flanked by 2 *LoxP* sites, followed by an enhanced GFP (green fluorescent protein) fused with human histone *H2B* gene for nuclear expression of GFP. Since the knock-in cassettes are promoterless, nlacZ or H2B-GFP (histone 2B fused GFP) expression is fully controlled by the endogenous *Myh11* gene, while H2B-GFP expression is not activated unless the *nlacZ-4XpolyA* cassette is removed by Cre-mediated recombination. Targeted ES cells were identified by long-range polymerase chain reaction amplification (Figure IB in the Data Supplement). *Myh11*$^{nlacZ\text{-}H2B\text{-}GFP/+}$ knock-in mice were obtained after crossing *Myh11*$^{nlacZ\text{-}H2B\text{-}GFP\text{-}Neo/+}$ mice with Flippase mice to remove the neomycin selection cassette. Heterozygous *Myh11*$^{nlacZ\text{-}H2B\text{-}GFP/+}$ knock-in male and female mice develop normally without growth or breeding abnormalities when compared with their wild-type littermates.

To determine if nlacZ expression in *Myh11*$^{nlacZ\text{-}H2B\text{-}GFP/+}$ mice faithfully marks SMCs, we collected tissues at embryonic and postnatal stages for X-gal staining. At E10.5, nlacZ positive cells (nlacZ$^+$) were detected in the umbilical cord of *Myh11*$^{nlacZ\text{-}H2B\text{-}GFP/+}$ embryos (Figure IIA through IIC in the Data Supplement). Sporadic nlacZ$^+$ cells were also seen within dorsal aorta, trachea, and esophagus (Figure IIB2 in the Data Supplement). At E14.5, nlacZ$^+$ cells were evident in the thoracic aorta, mesenteric artery, and gut (Figure 1B). At E16.5, nlacZ$^+$

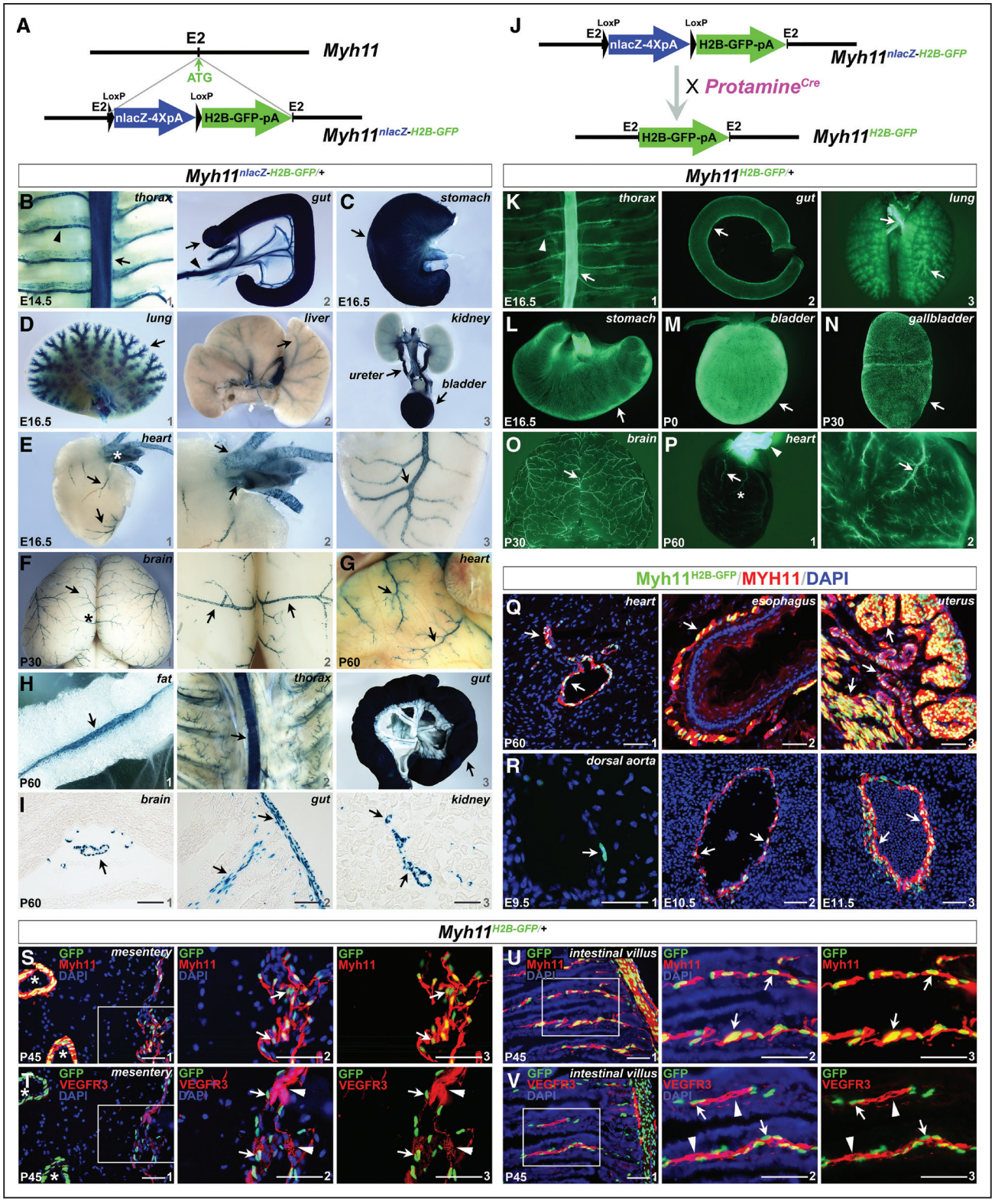

Figure 1. The expression of nuclear lacZ (nlacZ) and H2B-GFP (histone 2B fused green fluorescent protein) in the reporter mouse lines recapitulate endogenous Myh11 (myosin heavy chain 11) pattern.

A, Diagram shows strategy of generating *Myh11*$^{nlacZ\text{-}H2B\text{-}GFP}$ dual reporter mouse. **B**, X-gal staining shows Myh11^{nlacZ} expression in thoracic aorta (arrow in $\mathbf{B}_1$), intercostal artery (arrowhead in $\mathbf{B}_1$), gut (arrow in $\mathbf{B}_2$), and mesenteric artery (arrowhead in $\mathbf{B}_2$) at E14.5. **C**–**E**, Myh11^{nlacZ} expression in stomach (**C**), lung ($\mathbf{D}_1$), liver ($\mathbf{D}_2$), ureter and bladder ($\mathbf{D}_3$), aorta and pulmonary artery ($\mathbf{E}_{1,2}$), coronary vessels ($\mathbf{E}_3$) at E16.5. **F**, X-gal staining shows Myh11^{nlacZ} expression in blood vessels of brain at P30. Area marked by an asterisk in $\mathbf{E}_1$ and $\mathbf{F}_1$ is magnified in $\mathbf{E}_2$ and $\mathbf{F}_2$, respectively. **G** and **H**, Myh11^{nlacZ} expression in coronary artery (**G**), blood vessel of the adipose tissue ($\mathbf{H}_1$), thoracic aorta ($\mathbf{H}_2$), and gut ($\mathbf{H}_3$) at P60. **I**, Myh11^{nlacZ} expression in brain, gut, and kidney tissue sections. Arrows indicate nlacZ$^+$ cells. (*Continued*)

cells were specifically distributed in the stomach, airways in the lung, vasculature within the liver, ureter walls, bladder musculature, and in the walls of blood vessels throughout the embryo (Figure 1C and 1D). The nlacZ signals were also specifically seen in the coronary vessels and great arteries (aorta and pulmonary artery) at this stage (Figure 1E). At postnatal day 30 (P30) to adulthood (P60), nlacZ was continuously expressed in the blood vessels of various organs such as brain, heart, fat, thoracic aorta, and gut (Figure 1F through 1H). The nlacZ expression in SMCs was detected in both male and female mice (Figure IIIA and IIIB in the Data Supplement), and the genetic backgrounds between Black Swiss and C57BL/6J did not affect the specific expression (Figure IVA in the Data Supplement). We further sectioned tissues from brain, gut, and kidney and found nlacZ$^+$ cells are confined to the walls of vessels or hollow organs (Figure 1I). In *Myh11*$^{nlacZ\text{-}H2B\text{-}GFP/+}$ mice, H2B-GFP expression was undetectable in the SMCs of all organs examined. These observations reveal that nlacZ driven by endogenous *Myh11* promoter is specifically expressed in the presumptive SMCs localized in blood vessels and in the gastrointestinal and urinary tracts from embryonic stages to adulthood in *Myh11*$^{nlacZ\text{-}H2B\text{-}GFP/+}$ mice.

Myh11$^{H2B\text{-}GFP}$ Recapitulates Endogenous *Myh11* Expression

We next crossed *Myh11*$^{nlacZ\text{-}H2B\text{-}GFP/+}$ mice with *Protamine 1* promoter driven-Cre deleter mice (*Protamine*^{Cre})[12] to globally delete the *LoxP*-flanked *nlacZ* cassette to activate H2B-GFP expression in the nucleus (Figure 1J). In *Myh11*$^{H2B\text{-}GFP/+}$ mice, H2B-GFP is also under the control of endogenous *Myh11* promoter after removal of *nlacZ-4XpolyA* cassette (Figure IA in the Data Supplement).

We collected tissues from *Myh11*$^{H2B\text{-}GFP/+}$ mice for live imaging under fluorescent microscope. Similar to the findings revealed by the X-gal staining of *Myh11*$^{nlacZ\text{-}H2B\text{-}GFP/+}$ tissues, the GFP signal in umbilical cord was not detectable until E10.5 (Figure IID through IIF in the Data Supplement). At E16.5, robust nuclear GFP fluorescence (H2B-GFP$^+$) was detected in the thoracic aorta, gut, lung, and stomach, with patterns similar to the nlacZ expression in *Myh11*$^{nlacZ\text{-}H2B\text{-}GFP/+}$ mice (Figure 1K and 1L). Bright H2B-GFP signals were also observed in the hollow organs such as bladder and gallbladder at P0–30 (Figure 1M and 1N), and in the blood vessels of brain and coronary arteries of heart from P30 to adulthood (P30–60; Figure 1O and 1P). To define whether Myh11$^{H2B\text{-}GFP}$ recapitulates endogenous *Myh11* expression in SMCs, we sectioned adult mouse (P60) heart, esophagus, uterus (Figure 1Q), and aorta, gut, lung, spleen, vas deferens (Figure IIIE and IIIF in the Data Supplement) for immunostaining with antibody against MYH11. It showed that H2B-GFP and endogenous MYH11 expression were largely overlapped in all organs examined. The SMC-specific expression pattern of H2B-GFP is consistent in both sexes in Black Swiss or C57BL/6J genetic background (Figure IIIC through IIIF and IVB through IVE in the Data Supplement).

Direct visualization of H2B-GFP also revealed that Myh11 started expressing as early as E9.5 in dorsal aorta while MYH11 immunofluorescence staining failed to detect the Myh11$^+$ cells at this stage (Figure 1R-1). From E10.5 to E11.5, H2B-GFP signal is co-stained with a selected MYH11 antibody in the dorsal aorta (Figure 1R-2 and 1R-3 and Figure VA in the Data Supplement), yet other source MYH11 antibodies fail to detect these cells although they can stain adult SMCs (Figure VB through VF in the Data Supplement). We also found H2B-GFP faithfully marked SMCs of lymphatic vessels in mesentery and intestine at P45 (Figure 1S through 1V). Taken together, H2B-GFP signals in *Myh11*$^{H2B\text{-}GFP/+}$ mice not only can specifically identify SMCs that are of Myh11$^+$, but also can provide a more sensitive reporter for identification of SMCs than conventional immunostaining with MYH11 antibody.

Application of *Myh11*$^{nlacZ\text{-}H2B\text{-}GFP/+}$ Dual Reporter Mice to Trace Neural Crest and Second Heart Field-Derived SMCs in Heart

Previous studies have shown that *Wnt1*$^+$ neural crest progenitor cells contribute to SMCs in the aortic arch region of mice.[13] To demonstrate the proof of principle that *Myh11*$^{nlacZ\text{-}H2B\text{-}GFP/+}$ mice can be used to trace the origins of SMCs during development, we crossed *Myh11*$^{nlacZ\text{-}H2B\text{-}GFP/+}$ mice with *Wnt1*^{Cre} mice[14] (Figure 2A). With a combination of X-gal

Figure 1 Continued. J, Strategy for generating *Myh11*$^{H2B\text{-}GFP/+}$ reporter mice by crossing *Myh11*$^{nlacZ\text{-}H2B\text{-}GFP/+}$ mice with germline deleter *Protamine*^{Cre}. **K–M**, Direct visualization of Myh11$^{H2B\text{-}GFP}$ expression in thoracic aorta (arrow) and intercostal artery (arrowhead; **K**$_1$), gut (**K**$_2$), lung (**K**$_3$), stomach (**L**) at E16.5, and in bladder (**M**) at P0. **N–P**, Myh11$^{H2B\text{-}GFP}$ expression in gallbladder (**N**), blood vessels of brain (**O**) at P30. **P**, Myh11$^{H2B\text{-}GFP}$ expression in great arteries (arrowhead in **P**$_1$) and coronary vessels (arrows in **P**$_{1,2}$) at P60. The area marked by asterisk in **P**$_1$ is magnified on the right (**P**$_2$). **Q**, H2B-GFP (green) and immunostaining with MYH11 antibody (red, Abcam No. ab53219) in the coronary artery wall (**Q**$_1$), smooth muscles of esophagus (**Q**$_2$), and uterus (**Q**$_3$) at P60. DAPI was used to counter stain nucleus. **R**, H2B-GFP$^+$ cells and MYH11 antibody co-staining (Abcam No. ab53219) in the dorsal aorta of *Myh11*$^{H2B\text{-}GFP/+}$ mice at E9.5 (**R**$_1$), E10.5 (**R**$_2$), and E11.5 (**R**$_3$). Arrows indicate H2B-GFP$^+$ smooth muscle cells (SMCs). Separate layers of R$_2$ are also shown in Figure VA in the Data Supplement. **S–V**, *Myh11*$^{H2B\text{-}GFP/+}$ intestine tissues at P45 were immunostained with antibodies to MYH11 (**S** and **U**) and VEGFR3 (vascular endothelial growth factor receptor 3; **T** and **V**). **S/T** and **U/V** are consecutive sections. H2B-GFP and MYH11 were not only co-expressed on the wall of blood vessels (asterisks in **S**$_1$), but also co-expressed in the mesenteric collecting lymphatic vessels (arrows in **S**$_{2,3}$) that are VEGFR3$^+$ (arrowheads in **T**$_2$ and **T**$_3$). In intestinal villi, H2B-GFP and MYH11 were co-localized in the villus SMCs (arrows in **U**$_2$ and **U**$_3$) associated with lacteals that are VEGFR3$^+$ (arrowheads in **V**$_2$ and **V**$_3$). S$_{2/3}$, T$_{2/3}$, U$_{2/3}$, and V$_{2/3}$ are magnified boxed areas in **S**$_1$, **T**$_1$, **U**$_1$, and **V**$_1$, respectively. Scale bar, 50 μm.

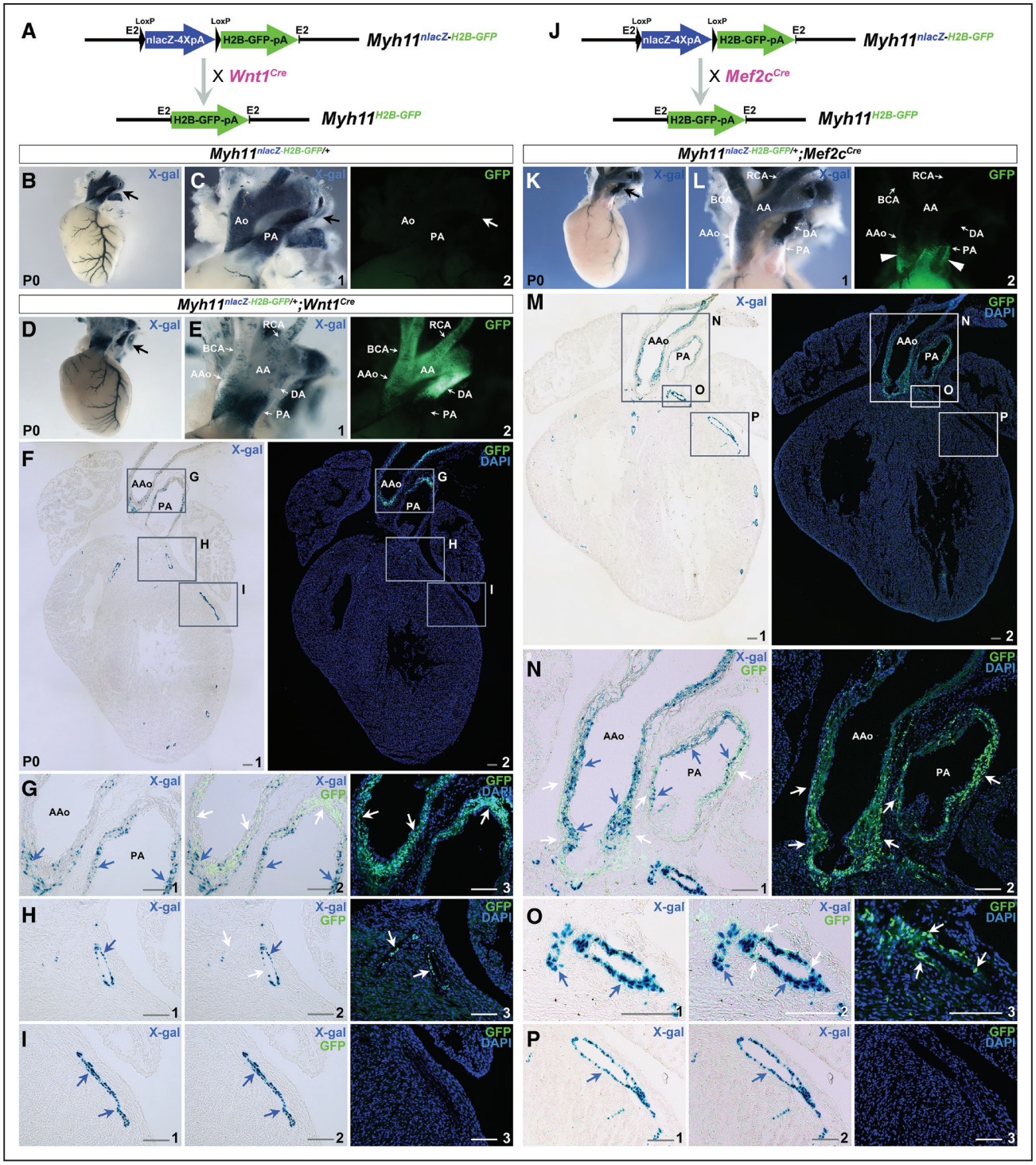

Figure 2. Heterogeneous origins of smooth muscle cells (SMCs) in the coronary vessels and great arteries revealed by *Myh11*$^{nlacZ\text{-}H2B\text{-}GFP/+}$;*Wnt1*^{Cre} and *Myh11*$^{nlacZ\text{-}H2B\text{-}GFP/+}$;*Mef2c*^{Cre} mice.

A, Diagram shows strategy of generating *Myh11*$^{nlacZ\text{-}H2B\text{-}GFP/+}$;*Wnt1*^{Cre} mice in which GFP (green fluorescent protein) is expected to be expressed in SMCs of neural crest origin. **B**–**E**, Whole-mount X-gal staining and GFP fluorescence imaging on *Myh11*$^{nlacZ\text{-}H2B\text{-}GFP/+}$ heart (**B** and **C**) and *Myh11*$^{nlacZ\text{-}H2B\text{-}GFP/+}$;*Wnt1*^{Cre} heart (**D** and **E**) at P0. While robust nuclear lacZ (nlacZ)-expressing cells were detected in all aortic tissues of *Myh11*$^{nlacZ\text{-}H2B\text{-}GFP/+}$ hearts (**C**$_1$), no GFP$^+$ cells were detected in these animals (**C**$_2$). In *Myh11*$^{nlacZ\text{-}H2B\text{-}GFP/+}$;*Wnt1*^{Cre} hearts, GFP signals were seen in neural crest-derived SMCs of distal ascending aorta (AAo), aortic arch (AA), brachiocephalic artery (BCA), right carotid arteries (RCA), and ductus arteriosus (DA), whereas the rest of SMCs are nlacZ$^+$ including pulmonary artery (PA) and AAo around aortic root (**D** and **E**). **F**, Longitudinal sections of *Myh11*$^{nlacZ\text{-}H2B\text{-}GFP/+}$;*Wnt1*^{Cre} neonatal heart after X-gal staining (**F**$_1$) and DAPI counterstaining with GFP (**F**$_2$). **G**–**I**, Magnified boxed areas in **F**. They show complementary nlacZ (blue arrows) and GFP (white arrows) signals in the ascending aorta (AAo), pulmonary artery (PA; **G**), and coronary artery close to aortic root (**H**). The coronary vessels distal to aortic root is fully contributed by nlacZ$^+$ but not GFP$^+$ cells (**I**). **J**, Diagram of generating *Myh11*$^{nlacZ\text{-}H2B\text{-}GFP/+}$;*Mef2c*^{Cre} mice in which GFP is expected to be (*Continued*)

staining and direct visualization of GFP, the neonatal *Myh11*$^{nlacZ\text{-}H2B\text{-}GFP/+}$ control mice (*Wnt1*^{Cre} negative) showed no expression of GFP while nlacZ marks virtually all SMCs in the aortic arch and coronary artery (Figure 2B and 2C). In contrast, *Wnt1*^{Cre} and *Myh11*$^{nlacZ\text{-}H2B\text{-}GFP/+}$ double-positive hearts (*Wnt1*^{Cre};*Myh11*$^{nlacZ\text{-}H2B\text{-}GFP/+}$) only exhibited specific GFP expression in the distal region of ascending aorta, brachiocephalic artery, subclavian artery, aortic arch, common carotid arteries, and ductus arteriosus. In these mice, the nlacZ$^+$ SMCs that were not Wnt1-expressing cell derived remained around the aortic root and pulmonary artery, consistent with these SMCs being derived from the second heart field (Figure 2D and 2E).[13,15] We sectioned the hearts for a thorough examination of GFP$^+$ and nlacZ$^+$ cells in different regions. This analysis revealed that there were a mixture of neural crest- and non-neural crest-derived SMC populations within both ascending aorta and pulmonary artery (Figure 2F and 2G). Interestingly, we found that SMCs within the coronary artery close to the aortic root also contain both GFP$^+$ and nlacZ$^+$ cells (Figure 2H), whereas coronary artery distal to aortic root, the SMCs are solely labeled by nlacZ (Figure 2I), suggesting a heterogenous origins of coronary SMCs in different regions of heart.

To rule out the potential insufficient recombination driven by *Wnt1*^{Cre}, we further crossed *Myh11*$^{nlacZ\text{-}H2B\text{-}GFP/+}$ *mice with Mef2c*^{Cre} mice[16] to visualize second heart field-derived SMCs in the heart (Figure 2J). By examining *Myh11*$^{nlacZ\text{-}H2B\text{-}GFP/+}$;*Mef2c*^{Cre} mice at birth, we found GFP$^+$ cells are largely located in the proximal ascending aorta and pulmonary artery (Figure 2K and 2L). Histological analysis showed that they were mainly around the aortic root and pulmonary artery, with complementary pattern to the nlacZ$^+$ SMCs that presumably derived from neural crest[13,15] (Figure 2M and 2N). Second heart field-derived GFP$^+$ progenies were also detected in the coronary artery close to aortic root (Figure 2O), but not in the coronary artery distal to aortic root (Figure 2P), further suggesting the heterogenous origins of SMCs in the coronary artery in mice. Taken together, our data show that the *Myh11*$^{nlacZ\text{-}H2B\text{-}GFP/+}$ dual reporters not only recapitulate endogenous *Myh11* expression to label SMCs at different stages, but also provides an exceptionally useful tool to explore the developmental origins of SMCs.

DISCUSSION

SMCs are important component of blood vessels and hollow organs. Definitive identification of SMCs is critical for understating their functions in vivo. Previously, smooth muscle-selective reporter mouse models have largely relied on transgenic approaches.[17–20] A grave concern on these models is that the random transgenic integrations may affect reporter expression and thereby not fully mimic endogenous SMC expression. This matter is exemplified by the current widely used *Myh11-CreER*^{T2} transgenic line with which only the male mice can be used as the transgene was unfavorably inserted into the Y chromosome.[21] The lacZ and GFP in our new *Myh11*$^{nlacZ\text{-}H2B\text{-}GFP/+}$ knock-in mouse model faithfully mirrors endogenous *Myh11* expression. Since both *Myh11*^{nlacZ} and *Myh11*$^{H2B\text{-}GFP}$ reporters are expressed in the nuclei of SMCs which have a much smaller volume than the cytoplasm where endogenous MYH11 protein is distributed, this design significantly increases the sensitivity of detection over the endogenous MYH11 protein. The *Myh11*$^{nlacZ\text{-}H2B\text{-}GFP/+}$ dual reporter mice thus offer an exceptional genetic tool that dramatically improves sensitivity and accuracy in detection and even quantification of SMCs in both male and female mice.

SMCs in different vessels or different zones of the same vessel may have distinct developmental origins.[22] In adults, the new SMCs can be generated from proliferation of the preexisting SMCs and through differentiation of the progenitor cells upon vascular injury.[23,24] Currently, it is uncertain what the relative contribution of progenitor cells versus preexisting SMCs are to the complement of adult SMCs and during regeneration following injury in SMC-enriched organs. A unique design of this dual reporter mouse line is that the *nlacZ* cassette is flanked by 2 *LoxP* sites followed by *H2B-GFP*. We can, therefore, cross the *Myh11*$^{nlacZ\text{-}H2B\text{-}GFP/+}$ mice to a progenitor specific-Cre expressing line to permit us to distinguish SMCs that are derived from the progenitor cells from those that are not. As we showed the heterogeneous origins of SMCs in coronary and great arteries using *Wnt1*^{Cre}, *Mef2c*^{Cre} and the dual reporter mouse lines (Figure 2), SMCs can either be labeled with H2B-GFP that of neural crest lineage origin or second heart field origin. In contrast, with the *Wnt1*^{Cre};*mTmG* dual fluorescence mice we tested recently,[11] although GFP can label neural crest-derived progenies, the RFP signals were found in both non-SMCs and non-neural crest-derived SMCs in these animals.

The *Myh11*$^{nlacZ\text{-}H2B\text{-}GFP/+}$ mouse line can also cross to an SMC-inducible Cre line to label all the preexisting SMCs (which are H2B-GFP$^+$) if Cre expression can be sufficiently induced in preexisting SMCs. This will eventually

Figure 2 Continued. expressed in second heart field-derived SMCs. **K** and **L**, Whole-mount X-gal staining and GFP fluorescence imaging of *Myh11*$^{nlacZ\text{-}H2B\text{-}GFP/+}$;*Mef2c*^{Cre} heart at P0. The nlacZ$^+$ cells were detected in distal ascending aorta (AAo), aortic arch (AA), brachiocephalic artery (BCA), RCA, and ductus arteriosus (DA; **L**$_1$, arrows). GFP$^+$ cells derived from *Mef2c*^{Cre} lineage were detected in the proximal ascending aorta (AAo) and pulmonary artery (PA; **L**$_2$, arrowheads). **M**, The nlacZ$^+$ (**M**$_1$) and GFP$^+$ cells with DAPI staining (**M**$_2$) on longitudinal sections of *Myh11*$^{nlacZ\text{-}H2B\text{-}GFP/+}$;*Mef2c*^{Cre} heart at P0. **N**–**P**, High magnification of the boxed areas in **M**. GFP$^+$ cells (white arrows) derived from *Mef2c*^{Cre} lineage were largely located in the outer media of ascending aorta (AAo) and pulmonary artery (PA), while nlacZ$^+$ cells (blue arrows) were mainly detected in the inner media (**N**$_1$). GFP$^+$ and nlacZ$^+$ cells were interspersed in the coronary artery close to aortic root (**O**). No GFP$^+$ cells derived from *Mef2c*^{Cre} lineage were detected in the distal left coronary artery (**P**). Scale bar, 100 μm. H2B-GFP indicates histone 2B fused GFP.

aid us to distinguish SMC populations which are generated de novo (nlacZ$^+$/H2B-GFP$^-$) from those arising from the preexisting SMCs (H2B-GFP$^+$/LacZ$^-$). In addition, the *Myh11*$^{nlacZ\text{-}H2B\text{-}GFP/+}$ mice can be applied to determine vascular wall development by crossing them with an inducible Cre line. Induction of these animals with low dosage of tamoxifen will help to decipher mechanisms of vascular SMC organization by clonal analysis of the labeled H2B-GFP$^+$ cells.

In summary, the *Myh11*$^{nlacZ\text{-}H2B\text{-}GFP/+}$ knock-in reporter mouse line described in this study offers a robust genetic tool not only to monitor *Myh11* expression, but when combined with specific-Cre drivers also to trace SMC origins under physiological and pathological conditions.

ARTICLE INFORMATION

Received July 27, 2020; accepted December 9, 2020.

Affiliations

School of Life Sciences, Shanghai University, China (J.R., F.C.). Department of Pediatrics, Herman Wells Center for Pediatric Research, Indiana University School of Medicine (J.R., L.Z., D.H., F.Y., M.S., C.S., W.S., C.-L.C.). Division of Pediatrics Cardiology, Vanderbilt University, Nashville, TN (X.Q.). Department of Pharmacology & Toxicology, Medical College of Georgia, Augusta University (X.H., J.S., K.D., J.Z.). Division of Cardiovascular Surgery, University of Maryland School of Medicine, Baltimore (D.L.).

Acknowledgments

We thank Drs Joseph Miano and B. Paul Herring for a critical reading of the article.

Sources of Funding

C.-L. Ca is supported by seed fund from Indiana University School of Medicine. J. Zhou is a recipient of Established Investigator Award (17EIA33460468) and Transformational Project Award (19TPA34910181) from the American Heart Association. K. Dong is supported by a postdoctoral fellowship (19POST34450071) from the American Heart Association.

Disclosures

None.

REFERENCES

1. Cheng JK, Wagenseil JE. Extracellular matrix and the mechanics of large artery development. *Biomech Model Mechanobiol.* 2012;11:1169–1186. doi: 10.1007/s10237-012-0405-8
2. Owens GK, Kumar MS, Wamhoff BR. Molecular regulation of vascular smooth muscle cell differentiation in development and disease. *Physiol Rev.* 2004;84:767–801. doi: 10.1152/physrev.00041.2003
3. Bentzon JF, Weile C, Sondergaard CS, Hindkjaer J, Kassem M, Falk E. Smooth muscle cells in atherosclerosis originate from the local vessel wall and not circulating progenitor cells in ApoE knockout mice. *Arterioscler Thromb Vasc Biol.* 2006;26:2696–2702. doi: 10.1161/01.ATV.0000247243.48542.9d
4. Tang J, Wang H, Huang X, Li F, Zhu H, Li Y, He L, Zhang H, Pu W, Liu K, et al. Arterial Sca1+ vascular stem cells generate de novo smooth muscle for artery repair and regeneration. *Cell Stem Cell.* 2020;26:81.e4–96.e4. doi: 10.1016/j.stem.2019.11.010
5. Babij P, Kelly C, Periasamy M. Characterization of a mammalian smooth muscle myosin heavy-chain gene: complete nucleotide and protein coding sequence and analysis of the 5' end of the gene. *Proc Natl Acad Sci USA.* 1991;88:10676–10680. doi: 10.1073/pnas.88.23.10676
6. Renard M, Callewaert B, Baetens M, Campens L, MacDermot K, Fryns JP, Bonduelle M, Dietz HC, Gaspar IM, Cavaco D, et al. Novel MYH11 and ACTA2 mutations reveal a role for enhanced TGFβ signaling in FTAAD. *Int J Cardiol.* 2013;165:314–321. doi: 10.1016/j.ijcard.2011.08.079
7. Albornoz G, Coady MA, Roberts M, Davies RR, Tranquilli M, Rizzo JA, Elefteriades JA. Familial thoracic aortic aneurysms and dissections–incidence, modes of inheritance, and phenotypic patterns. *Ann Thorac Surg.* 2006;82:1400–1405. doi: 10.1016/j.athoracsur.2006.04.098
8. Kloth K, Renner S, Burmester G, Steinemann D, Pabst B, Lorenz B, Simon R, Kolbe V, Hempel M, Rosenberger G. 16p13.11 microdeletion uncovers loss-of-function of a MYH11 missense variant in a patient with megacystis-microcolon-intestinal-hypoperistalsis syndrome. *Clin Genet.* 2019;96:85–90. doi: 10.1111/cge.13557
9. Alhopuro P, Phichith D, Tuupanen S, Sammalkorpi H, Nybondas M, Saharinen J, Robinson JP, Yang Z, Chen LQ, Orntoft T, et al. Unregulated smooth-muscle myosin in human intestinal neoplasia. *Proc Natl Acad Sci USA.* 2008;105:5513–5518. doi: 10.1073/pnas.0801213105
10. Yan J, Zhang L, Sultana N, Oh JG, Wu B, Hajjar RJ, Zhou B, Cai CL. A series of robust genetic indicators for definitive identification of cardiomyocytes. *J Mol Cell Cardiol.* 2016;97:278–285. doi: 10.1016/j.yjmcc.2016.06.003
11. Osman I, Wang L, Hu G, Zheng Z, Zhou J. GFAP (Glial Fibrillary Acidic Protein)-positive progenitor cells contribute to the development of vascular smooth muscle cells and endothelial cells-brief report. *Arterioscler Thromb Vasc Biol.* 2020;40:1231–1238. doi: 10.1161/ATVBAHA.120.314078
12. O'Gorman S, Dagenais NA, Qian M, Marchuk Y. Protamine-Cre recombinase transgenes efficiently recombine target sequences in the male germ line of mice, but not in embryonic stem cells. *Proc Natl Acad Sci USA.* 1997;94:14602–14607. doi: 10.1073/pnas.94.26.14602
13. Jiang X, Rowitch DH, Soriano P, McMahon AP, Sucov HM. Fate of the mammalian cardiac neural crest. *Development.* 2000;127:1607–1616.
14. Danielian PS, Muccino D, Rowitch DH, Michael SK, McMahon AP. Modification of gene activity in mouse embryos in utero by a tamoxifen-inducible form of Cre recombinase. *Curr Biol.* 1998;8:1323–1326. doi: 10.1016/s0960-9822(07)00562-3
15. Sawada H, Rateri DL, Moorleghen JJ, Majesky MW, Daugherty A. Smooth muscle cells derived from second heart field and cardiac neural crest reside in spatially distinct domains in the media of the ascending aorta-brief report. *Arterioscler Thromb Vasc Biol.* 2017;37:1722–1726. doi: 10.1161/ATVBAHA.117.309599
16. Verzi MP, McCulley DJ, De Val S, Dodou E, Black BL. The right ventricle, outflow tract, and ventricular septum comprise a restricted expression domain within the secondary/anterior heart field. *Dev Biol.* 2005;287:134–145. doi: 10.1016/j.ydbio.2005.08.041
17. Li L, Miano JM, Mercer B, Olson EN. Expression of the SM22alpha promoter in transgenic mice provides evidence for distinct transcriptional regulatory programs in vascular and visceral smooth muscle cells. *J Cell Biol.* 1996;132:849–859. doi: 10.1083/jcb.132.5.849
18. Madsen CS, Regan CP, Hungerford JE, White SL, Manabe I, Owens GK. Smooth muscle-specific expression of the smooth muscle myosin heavy chain gene in transgenic mice requires 5'-flanking and first intronic DNA sequence. *Circ Res.* 1998;82:908–917. doi: 10.1161/01.res.82.8.908
19. Smith AF, Bigsby RM, Word RA, Herring BP. A 310-bp minimal promoter mediates smooth muscle cell-specific expression of telokin. *Am J Physiol.* 1998;274:C1188–C1195; discussion C1187. doi: 10.1152/ajpcell.1998.274.5.C1188
20. Xin HB, Deng KY, Rishniw M, Ji G, Kotlikoff MI. Smooth muscle expression of Cre recombinase and eGFP in transgenic mice. *Physiol Genomics.* 2002;10:211–215. doi: 10.1152/physiolgenomics.00054.2002
21. Wirth A, Benyó Z, Lukasova M, Leutgeb B, Wettschureck N, Gorbey S, Orsy P, Horváth B, Maser-Gluth C, Greiner E, et al. G12-G13-LARG-mediated signaling in vascular smooth muscle is required for salt-induced hypertension. *Nat Med.* 2008;14:64–68. doi: 10.1038/nm1666
22. Hirschi KK, Majesky MW. Smooth muscle stem cells. *Anat Rec A Discov Mol Cell Evol Biol.* 2004;276:22–33. doi: 10.1002/ar.a.10128
23. Majesky MW, Dong XR, Regan JN, Hoglund VJ. Vascular smooth muscle progenitor cells: building and repairing blood vessels. *Circ Res.* 2011;108:365–377. doi: 10.1161/CIRCRESAHA.110.223800
24. Psaltis PJ, Simari RD. Vascular wall progenitor cells in health and disease. *Circ Res.* 2015;116:1392–1412. doi: 10.1161/CIRCRESAHA.116.305368